

## Value of quantitative apparent diffusion coefficients in differentiating low-grade gliomas from mixed neuronal-glia tumors



Amit Agarwal<sup>a,\*</sup>, Sangam Kanekar<sup>b</sup>, Shyam Sabat<sup>c</sup>, Girish Bathla<sup>d</sup>

<sup>a</sup> Mayo Clinic, 4500 San Pablo Road, Jacksonville, FL, 32224, USA

<sup>b</sup> Department of Neurology & Radiology, Penn State University, Hershey, PA, 17033, USA

<sup>c</sup> University of Florida, Gainesville, 1600 SW Archer Rd, Gainesville, FL, 32611, USA

<sup>d</sup> Clinical Neuroradiology Research, University of Iowa Hospitals and Clinics, Iowa City, IO, USA

### ARTICLE INFO

#### Keywords:

Diffusion-weighted imaging (DWI)  
Apparent diffusion coefficient (ADC)  
Low-grade gliomas (LGGs)  
Mixed neuronal and glial tumors (MNGTs)

### ABSTRACT

**Purpose:** To retrospectively assess if diffusion-weighted MR imaging (DWI) and quantitative apparent-diffusion coefficient (ADC) maps could be used to differentiate between low-grade gliomas (LGGs) and mixed neuronal-glia tumors (MNGTs including Dysembryoplastic Neuroepithelial Tumor and Ganglioglioma).

**Materials and methods:** We retrospectively searched the clinical, pathological, and radiological databases for a span of 9 years and identified 24 patients with biopsy proven LGG. This included WHO (fourth edition) grade I and II tumors including astrocytoma, oligoastrocytoma and oligodendrogliomas. We also identified 22 patients with MNGTs (WHO grade I) including 13 patients with DNET and 9 patients with Ganglioglioma. All patients with pathologically confirmed tumors who had MRI including DWI sequence were included in the study. Regions of interest (ROIs) of 0.1–0.15 cm<sup>2</sup> were manually positioned on the ADC maps and multiple values (10<sup>-6</sup> mm<sup>2</sup>/s) were obtained including the ADC<sub>mean</sub>. Optimal thresholds of ADC values and ADC ratios for distinguishing low-grade gliomas from mixed neuronal-glia tumors were determined by receiver operating characteristic (ROC) curve analysis.

**Results:** All the four ADC measurement variables, including the minimum (ADC min), the (ADC max) maximum, the mean of ADC values (ADC mean) and the ADC ratios (ADC mean/ADC<sub>normal</sub>) showed significant difference between the MNGTs and LGGs. The most significant difference was seen with the maximum ADC value (ADC max) of the tumor where the values for LGGs were 1317 ± 314 whereas the values for MNGTs were 2134 ± 438. In both subsets of patients with MNGTs (DNET and Ganglioglioma), this difference was statistically significant (P = .015 and P = .0066, respectively). However, there was no significant difference between the ADC values of these subtypes of MNGTs.

**Conclusion:** The ADC values of MNGTs are significantly higher compared to LGGs and can be helpful in radiological demarcation of these two conditions. The high ADC of MNGTs may be attributable to the presence of large extracellular spaces and their cellularity, which is much lower than that of pure glial neoplasms.

### 1. Introduction

Accurate brain tumor diagnosis plays an essential role in the selection of the optimum treatment strategy, as the nature of the tumor and the grade defines the therapeutic approach. Advanced magnetic resonance imaging (MRI) techniques have added incremental diagnostic information regarding tumor characterization over conventional MRI. Particularly, diffusion weighted imaging (DWI) and diffusion tensor imaging (DTI) provide significant structural and functional information that

although macroscopic reflect the microscopic mechanisms of the underlying pathophysiology.<sup>1</sup> Diffusion-weighted MR imaging (DWI) and quantitative apparent diffusion coefficient (ADC) is increasingly being incorporated into standard clinical evaluation of brain tumors.

Gliomas are the most common brain tumors. On imaging studies, low-grade gliomas usually show little to no abnormal enhancement or peritumoral edema, except for pilocytic astrocytoma and giant-cell astrocytoma.<sup>2</sup> Mixed neuronal-glia tumors (MNGTs) are a pathologically distinct group of cortically based tumors commonly associated with medically intractable epilepsy. They are seen predominantly in young

\* Corresponding author.

E-mail addresses: [amitmamc@gmail.com](mailto:amitmamc@gmail.com), [agarwal.amit@mayo.edu](mailto:agarwal.amit@mayo.edu) (A. Agarwal), [skanekar@pennstatehealth.psu.edu](mailto:skanekar@pennstatehealth.psu.edu) (S. Kanekar), [shyamsundersabat@gmail.com](mailto:shyamsundersabat@gmail.com) (S. Sabat), [girish-bathla@uiowa.edu](mailto:girish-bathla@uiowa.edu) (G. Bathla).

<https://doi.org/10.1016/j.wnsx.2023.100159>

Received 7 June 2022; Accepted 19 January 2023

2590-1397/© 2023 The Authors. Published by Elsevier Inc. This is an open access article under the CC BY-NC-ND license (<http://creativecommons.org/licenses/by-nc-nd/4.0/>).

**Abbreviation list**

ADC	apparent-diffusion coefficient
LGGs	Low grade gliomas
MNGTs	mixed neuronal-glioma tumors
DNET	Dysembryoplastic Neuroepithelial Tumor
ROI	Region of interest
MRI	Magnetic resonance imaging
DWI	Diffusion weighted imaging
DTI	diffusion tensor imaging
WHO	World Health organization
TR	Time to repetition
TE	Echo time
FOV	Field of view
AUC	area under curve

adults and are characterized by drug resistant seizures and normal neurological examination. These are low-grade lesions in the WHO (fourth edition) classification of brain tumors, majority being grade I. On conventional MRI, superficial location, triangular or wedge-like appearance with internal septations and variable presence of contrast enhancement and calcification are well-described features. Unfortunately, low-grade glioma tumors can occur in similar locations, age group, and show similar MRI features. Although conventional sequences can help in demarcating these two types of tumors, many overlapping features exist, including cortical location, markedly hyperintense T2 signal with low T1 signal, which makes radiographic differentiation challenging. DWI with ADC values is increasingly being utilized to differentiate brain tumors, a great example being demarcation of medulloblastomas and posterior fossa ependymomas. Differentiation of mixed neuronal tumors from the more common glioma tumors is crucial because neuronal tumors have favorable clinical outcomes and are generally curable with total surgical resection alone, whereas gliomas typically require more extensive imaging follow-up, surgery, and further chemo-radiotherapy depending on their histologic grade and have poor long-term prognosis.<sup>3</sup>

Our retrospective investigation aimed to assess whether quantitative ADC values and ratios in the tumoral core could be used to differentiate LGGs from MNGTs.

## 2. Materials and methods

### 2.1. Patients and histopathological analysis

The University Institutional Review Board approved the study. We searched the clinical, pathological, and radiological databases for nine years to retrospectively identify 22 patients with MNGTs at our institution, a tertiary care University hospital and Cancer Institute. This included 13 patients (59%) with DNET and 9 (41%) with Ganglioglioma (mean age  $\pm$  SD  $15 \pm 11$  years, age range 7–39 years). Inclusion criteria included patients with pathologically confirmed tumors (grade I) who had MRI including DWI sequence were included in the study. Most common clinical presentation was epileptic seizures, and the median duration of epilepsy was 2 years at the time of surgery. All patients underwent lesionectomy with or without extended corticectomy. Diffusion-weighted images in 24 age-matched control patients with pathologically confirmed low-grade glioma were also examined (mean age  $\pm$  SD  $28 \pm 19$  years, age range 22–39 years). Operative pathology of LGGs revealed pure astrocytoma in 13 patients (54%), oligoastrocytoma in 6 (25%), and oligodendroglioma in 5 (21%). Exclusion criteria were predominantly cystic morphology, including pilocytic astrocytomas, and tumors with dense calcifications.

The presence of macrocystic changes and calcification would have spuriously elevated or decreased the ADC calculation.

### 2.2. Magnetic resonance (MR) imaging and diffusion-weighted MR imaging (DWI)

All MR images were obtained with a 1.5-T superconducting system (Magnetom Vision; Siemens Medical Systems, Erlangen, Germany) using a circularly polarized head coil. DWI images and conventional MRI images were obtained in all patients. Sagittal T1-weighted (T1WI) localizing images (TR/TE/NEX, 15/6/1) were acquired first, and then unenhanced axial T1WI and T2-weighted (T2WI) images were obtained in each patient. All conventional sequences were obtained with a 5-mm section thickness and a 1-mm intersection gap. DWI was performed before administration of contrast medium in the transverse plane by using a single-shot SE echo-planar sequence with the following parameters: TR/TE 3100/96 ms, matrix size  $128 \times 128$ , FOV 211 mm, slice thickness 5 mm, intersection gap 1.5 mm; diffusion gradient encoding in three orthogonal directions (x, y and, z axes) at b values of 0, 500, and 1000 s/mm<sup>2</sup>. From these data, ADC maps and values were calculated on a pixel-by-pixel basis by using a Syngo workstation (Siemens, Erlangen, Germany) operating with the regions of interest (ROIs).

### 2.3. Diffusion-weighted images and ADC map evaluation

For each patient, the solid (enhancing and non-enhancing) portion of the lesion was identified using a combination of T1, T2 FLAIR and postcontrast T1-weighted images and matching ADC maps. Regions of interest (ROIs) of 50–100 mm<sup>2</sup> were accordingly manually positioned at the PACS workstations (GE Centricity, Imagecast PACS: 10.7, USA) and all values were automatically calculated and expressed in 10<sup>-6</sup> mm<sup>2</sup>/s. The neuroradiologist placing the ROIs was blinded to the tumor histology. The first region of interest was placed over homogenous enhancing and/or solid appearing regions in the central portion of tumors. Three additional ROIs were placed on the solid areas on different sections, or, if the tumor was present on fewer than 4 sections, these ROIs were positioned so that overlapping with the first ROI was avoided. A total of 4 lesion ROIs were obtained and averaged to serve as the ADC tumor average value. Control ADC values (ADC<sub>n</sub>) were obtained by placing ROIs in the normal-appearing contralateral side of the brain (Fig. 1). The ROIs were carefully placed to avoid cystic, necrotic, and hemorrhagic regions that might influence ADC values. The minimum (ADC<sub>min</sub>), the (ADC<sub>max</sub>) maximum and the mean of ADC values (ADC<sub>mean</sub>) were tabulated for analysis. Additionally, ADC ratios were calculated by dividing the mean ADC values within the tumor with the ADC value in the contralateral normal brain (ADC<sub>mean</sub>/ADC<sub>n</sub>).

### 2.4. Statistical analysis

Statistical analysis was performed with a commercially available software package (Statview, version 5.0; SAS Institute, Cary, NC). Comparison of obtained normal brain and tumor ADC values was done by using a 2-tailed paired *t*-test, whereas comparison of ADC values and ratios among groups was performed with a 2-tailed unpaired *t*-test. The observed differences were considered statistically significant if P was less than 0.05. Optimal thresholds of ADC values and ADC ratios for distinguishing low-grade gliomas from mixed neuronal-glioma tumors were determined by receiver operating characteristic (ROC) curve analysis. The multifactorial logistic regression was done stepwise by taking the area under the curve (AUC). Sensitivity, specificity, positive (PPV), and negative predictive values (NPV) were tabulated.

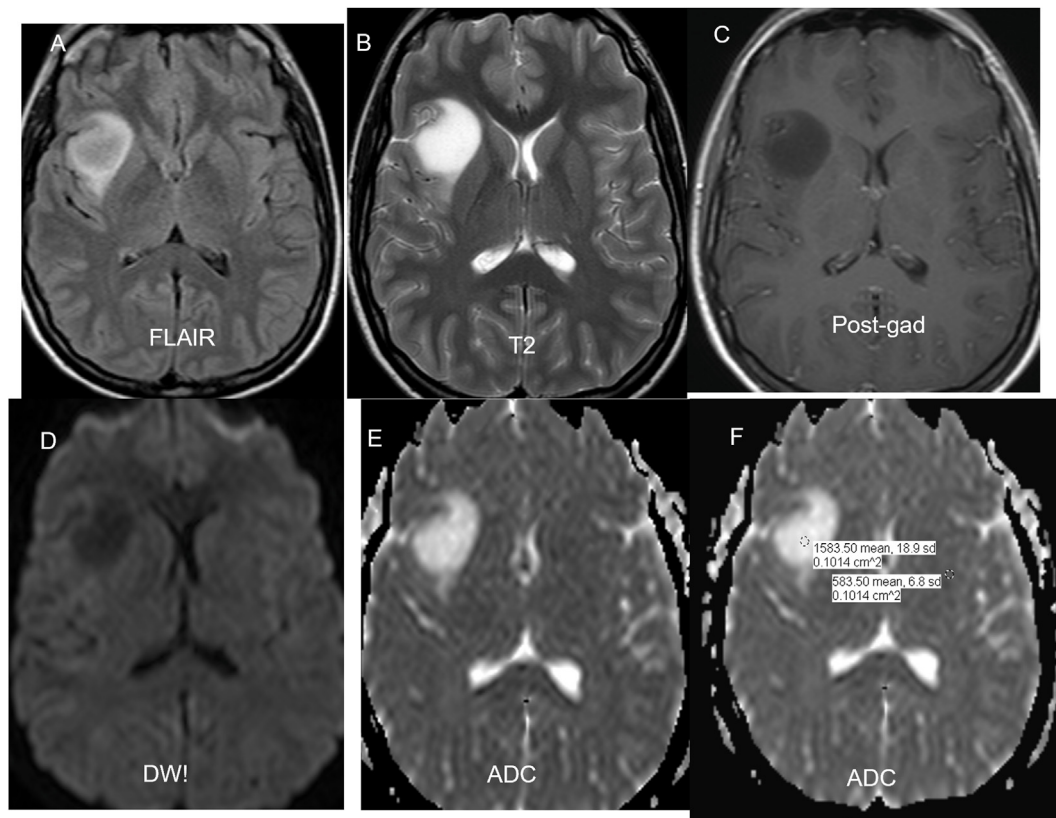


**Fig. 1.** Measurement of ADC values: FLAIR (a), T2 (b) and post-contrast (c) images are used to localize the best area for ADC value determination. Region of interest is localized within the tumor and contralateral white matter (f).

**3. Results**

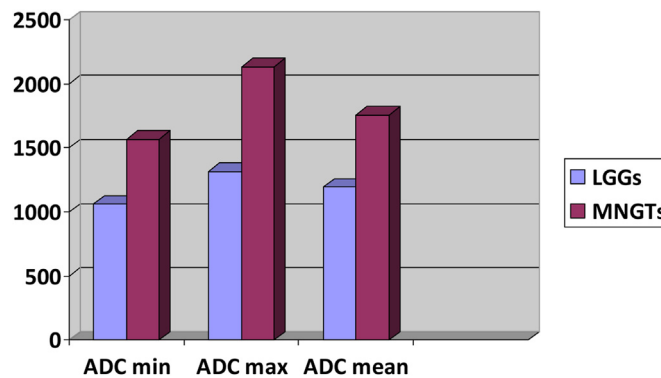
The results with various ADC values are summarized in [Table 1](#) and accompanying bar diagram. Normal brain ADC values among patients with LGGs and MNGTs were not significantly different ( $P = .82-0.89$ ). In patients with MNGTs, the average tumor ADC value versus normal brain versus was significantly different ( $P < .001$ ). In both subsets of patients

with MNGTs (DNET and Ganglioglioma), this difference was statistically significant ( $P = .015$  and  $P = .0066$ , respectively). However, there was no significant difference between the ADC values of these subtypes of MNGTs. There was no significant difference between the ADC values of LGGs and normal brain. Finally, the results showed that MNGTs and LGGs could be differentiated by using ADC values with significant statistical difference and p value less than 0.001. The MNGTs group showed

**Table 1**

Results and comparisons of ADC values and ratios in low-grade gliomas (LGGs) and Mixed Neuronal-gliomas (MNGTs).

ADC ( $10^{-6} \text{ mm}^2/\text{s}$ )	LGGs (n = 24)	MNGTs (n = 22)	P-value
ADC <sub>min</sub>	1062 ± 256	1567 ± 351	0.012
ADC <sub>max</sub>	1317 ± 314	2134 ± 438	0.006
ADC <sub>mean</sub>	1194 ± 173	1755 ± 250	0.009
ADC <sub>mean/n</sub>	2.11 ± 0.34	3.32 ± 0.47	0.021



Bar graph representing the ADC value (minimum, maximum and mean) comparison between LGGs and MNGTs.

ADC = apparent diffusion coefficient, mean/n = ADC ratios calculated by dividing the mean ADC values within the tumor with the ADC value in the contralateral normal brain.

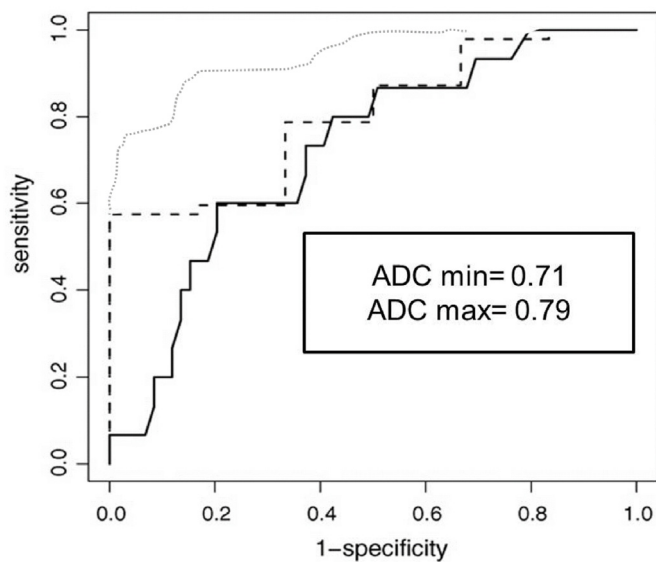


**Fig. 2.** Step-up ROC analyses on the potential multifactorial models lead to an optimal logistic regression model including the four factors: mean ADCt value and the minimum, maximum and mean ADCt ratio variables. The AUC of the combined four factors was 0.86.

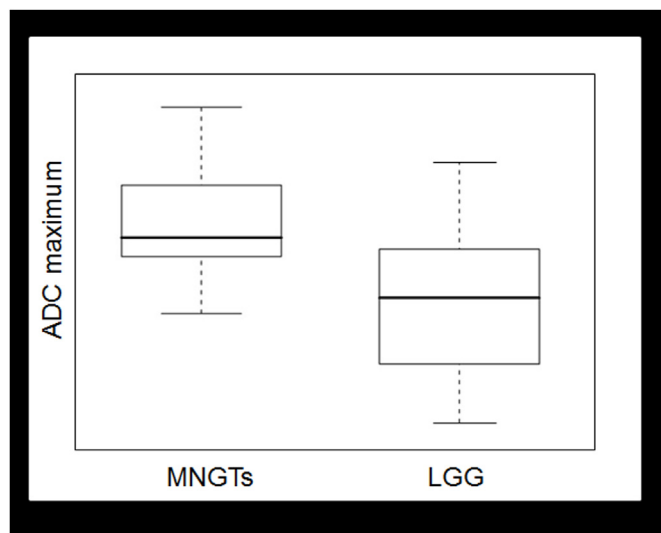


**Fig. 3.** Optimal cut-off value for differentiation of MNGTs from LGGs of 1824 (logistic regression fitted-value) which implies a sensitivity of 80.9%, a specificity of 71.6%.

significantly higher ADC values compared to LGGs.

All the four measurement variables, including the minimum ( $ADC_{min}$ ), the ( $ADC_{max}$ ) maximum, the mean of ADC values ( $ADC_{mean}$ ) and the ADC ratios ( $ADC_{mean}/ADC_n$ ) showed significant difference between the MNGTs and normal brain. None of these variables were significantly different when LGGs were compared to the normal brain. The most significant difference was seen with the maximum ADC value ( $ADC_{max}$ ) of the tumor.

The results of the ROC curve analysis are presented in Fig. 2, giving the sensitivity, specificity, PPV, NPV, accuracy and AUC for the different quantitative variables for distinguishing HGGs from LGGs. ROC analyses for each ADC-value as a single factor, found the maximum ADCt ratio to be the best predictive indicator. The AUC of this quantitative parameter was 0.73. The optimal cut-off value for differentiating MNGTs from LGGs was 1.350 (sensitivity 54.2%, specificity 91.3%, accuracy 64.6%) for minimum ADCt ratio (Table 1). Step-up ROC analyses on the potential

multifactorial models lead to an optimal logistic regression model including the four factors: mean ADCt value and the minimum, maximum and mean ADCt ratio variables. The AUC of the combined four factors was 0.86 (Fig. 3). We evaluated an optimal cut-off value for differentiation of MNGTs from LGGs of 1.824 (logistic regression fitted value) which implies a sensitivity of 80.9%, a specificity of 71.6%, and an accuracy of 75.6% (Fig. 3).

Thus, using the given model for a new patient, a probability value of more than the cut-off value predicts a MNGT, while a probability below the threshold suggests low-grade glioma. All four main parameters are significant on the 5% level in this model and thus contribute to the prediction. Examples of LGG and HGG using DWI are given in Fig. 4.

#### 4. Discussion

Diffusion-weighted imaging is an established valuable sequence for grading and characterizing tumors across the body ranging from prostatic neoplasm, renal, hepatic, and intracranial neoplasms. This is primarily related to the tumor cellularity with more cellular tumors having lesser free motion of water resulting in high DWI signal and low ADC values. However, there are other factors at play including the tumor matrix and composition.<sup>4,5</sup> The role of ADC values is well-established in literature for some tumors including extraaxial lesions like meningiomas and intracranial tumors like medulloblastomas and primary CNS lymphomas.<sup>6</sup> Medulloblastoma serves as a great example where the markedly low ADC values are helpful in demarcating them from ependymomas with values lower than 900 ( $10^{-6}$  mm<sup>2</sup>/s) being almost 100% specific for the former.<sup>7</sup> The utility of ADC maps has also been established for pre-operative grading of glial neoplasm. Apart from the areas of high tumor cellularity (low ADC) serving as an important marker for stereotactic biopsy, the wide range of variability within the tumors on the ADC maps also serves as a marker for higher grade. This is also relevant as in many cases the enhancing component of the tumor may not necessarily be the most malignant part of the tumor.<sup>8</sup> Using a combination of low ADC values and enhancement, together will result in much better neurosurgical target delineation and tissue sampling compared to either of these factors alone.<sup>9,10</sup> Despite significant overlap in ADC values of glial neoplasm, multiple studies have shown statistically significant difference in values between different subsets.<sup>11</sup> Higano *et al* in their study showed that the minimum ADC (834) of Glioblastoma was significantly lower than that (1060) of anaplastic astrocytoma with p-value less than 0.001.<sup>12</sup> Studies utilizing the role of ADC values in tumor characterization generally agree to the point that LGGs have higher values compared to high-grade glial neoplasm, secondary to moderate cellularity, loose intercellular connections, and wide extracellular space. Our results on the ADC values of LGGs were concordant with previous studies. As for example, our range of minimum to maximum ADC were from 1062 to 1317, was similar to the study by Bulakbasi *et al* where they compared the ADC values of LGGs with high-grade tumors.<sup>10,11</sup> Studies have also evaluated the role of ADC to assess for tumor response and to differentiate vasogenic edema for tumor infiltration in high-grade gliomas. In 2019, a study by Durand *et al* revealed statistically significant difference in ADC values in different tumor component including the necrotic, enhancing areas and finally between vasogenic edema and non-enhancing tumor components, both of which appear FLAIR hyperintense.<sup>13,14</sup>

We hypothesized that the ADC values of MNGTs are higher than that of LGGs which is consistent with histological make-up of the tumor. The high ADC of MNGTs may be attributable to the presence of large extracellular spaces and their cellularity, which is much lower than that of other brain tumors (Fig. 5).<sup>15</sup> These tumors belong to the one end of spectrum with high ADC values, the other end occupied by dense cellular tumors like medulloblastomas, initially classified under the umbrella term of “blue-cell” tumors. Limited studies on the ADC values of MNGTs have shown that these tumors have the highest values among all parenchymal neoplasm except for cystic neoplasms like juvenile pilocytic

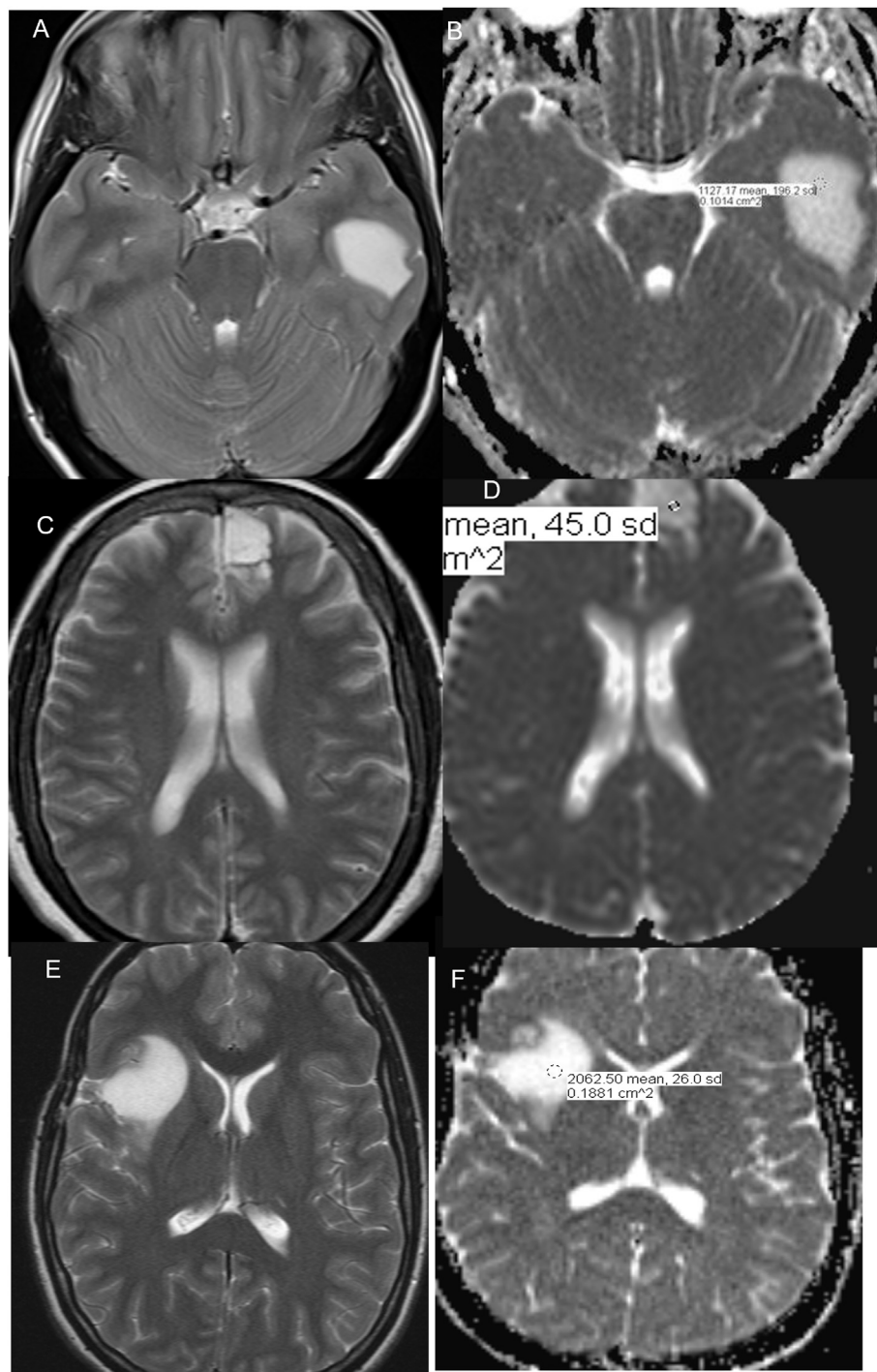


**Fig. 4.** Multiple T2 and corresponding ADC images in LGGs (a,b), ganglioglioma (c,d) and DNETs (e,f) show the gradient increase in ADC values with highest values seen in DNETs.

astrocytoma.<sup>2,16</sup> This is followed by LGGs, ependymomas, high-grade glial neoplasm and finally the dense “blue-cell” tumors like medulloblastoma. Intratumoral heterogeneity was highest for ependymomas and glioblastomas primarily due to the presence of cystic and necrotic components, respectively. Inflammatory conditions, like encephalitis can sometime mimic these tumors, however they tend to be diffuse with primarily gyriform signal changes and “band-like” cortical restricted diffusion (low ADC values). Tumefactive perivascular spaces also form a great radiologic differential to MNGTs and can be easily mistaken for neoplasms. These are however characterized by cluster of uniform or

variable-sized cysts which follow CSF signal on all sequences and are arranged in a radial pattern along the direction of the vessels. Relatively recently described lesions like multinodular and vacuolating neuronal tumors (MVNT) can also mimic MNGTs on imaging due to their multi-cystic (“bubbly”) appearance, however are classically located in the juxtacortical white matter, rather than in the cortex. The one major limitation of our study is the presence of cystic components within DNETs and gangliogliomas which may artificially elevate the ADC measurements. Although, we excluded cases with macrocystic changes, the presence of microcystic changes is poorly discernible on basic

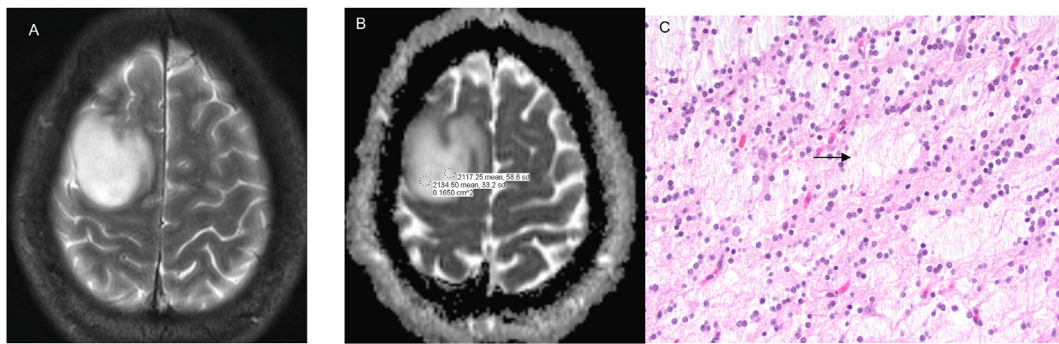


**Fig. 5.** Frontal lobe DNET with T2 (a) and ADC map showing the hyperintense lesion with high ADC value (2100–2300). The high ADC of DNETs may be attributable to the presence of large extracellular spaces and their cellularity as seen on histopathology (c). The black arrow depicts the large extracellular matrix on the H&E stained slide.

sequences like T2W and FLAIR. Nevertheless, these microcystic changes in fact might be the very cause of high ADC values of these MNGTs and may provide a good explanation for difference with LGGs as both have similar large extracellular spaces on histopathology. Another limitation of our study was the exclusion of cystic LGGs like pilocytic astrocytoma which have ADC values almost similar to CSF. Despite these limitations, we find the ADC maps to be a very useful tool in the radiologic characterization of any brain neoplasm. Moreover, DWI is an inherent part of any brain MRI and ADC values are easily measurable. Automated software are now available to provide a voxel-base three-dimensional mean of tumor ADC values making it an easy parameter to evaluate.<sup>17</sup> Although, our studies did not find a statically significant difference between DNETs and gangliogliomas, few studies available have shown that DNETs might have the highest ADC values among all parenchymal neoplasm. Larger studies are needed to further characterize the different tumors under the MNGTs umbrella on DWI. Finally, the new fifth edition of the WHO central nervous tumor classification was recently released with much stronger focus on the molecular markers and genetic signature of tumors. Radiographic segregation of the different molecular subtypes is at an early stage with the current radiologic focus still being differentiation of low-grade gliomas, high grade gliomas and mixed-glioneuronal tumors.<sup>18</sup>

## 5. Conclusion

The ADC value, minimal ADC value, and ADC ratios of solid tumoral or enhancing region appeared to be useful for differentiating low-grade tumors from mixed neuronal tumors. An ADC mean cut-off value of 1800 can be used as a benchmark for this with around 80% sensitivity.

## Credit author

Amit Agarwal: Conceptualization, IRB approval, Manuscript, data collection, Writing – original draft preparation, Sangam Kanekar, Data curation, Review and editing, Formal analysis, Shyam Sabat MD, Data curation, Review and editing, Formal analysis, Girish Bathla, Supervision, Review and editing.

## Declarations of competing interest

The authors declare that they have no conflict of interest.

## References

1. Svolos P, Tsolaki E, Kapsalaki E, et al. Investigating brain tumor differentiation with diffusion and perfusion metrics at 3T MRI using pattern recognition techniques. *Magn Reson Imaging*. 2013 Nov;31(9):1567–1577.
2. Kono K, Inoue Y, Nakayama K, et al. The role of diffusion-weighted imaging in patients with brain tumors. *AJNR Am J Neuroradiol*. 2001;22:1081–1088.
3. Parmar HA, Hawkins C, Ozelame R, et al. Fluid-attenuated inversion recovery ring sign as a marker of dysembryoplastic neuroepithelial tumors. *J Comput Assist Tomogr*. 2007 May-Jun;31(3):348–353.
4. Sugahara T, Korogi Y, Kochi M, et al. Use-fulness of diffusion-weighted MRI with echo-planar technique in the evaluation of cellularity in gliomas. *J Magn Reson Imaging*. 1999;9:53–60.
5. Messina C, Bignone R, Bruno A, et al. Diffusion-weighted imaging in oncology: an update. *Cancers*. 2020;12(6):1493.
6. Yamasaki F, Kurisu K, Satoh K, et al. Apparent diffusion coefficient of human brain tumors at MR imaging. *Radiology*. 2005;235:985–991.
7. Rumboldt Z, Camacho DL, Lake D, et al. Apparent diffusion coefficients for differentiation of cerebellar tumors in children. *AJNR Am J Neuroradiol*. 2006 Jun-Jul;27(6):1362–1369.
8. Lam WW, Poon WS, Metreweli C. Diffusion MR imaging in glioma: does it have any role in the pre-operation determination of grading glioma? *Clin Radiol*. 2002;57: 219–225.
9. Murakami R, Hirai T, Sugahara T, et al. Grading astrocytic tumors by using apparent diffusion coefficient parameters: superiority of a one- versus two-parameter pilot method. *Radiology*. 2009 Jun;251(3):838–845.
10. Bulakbasi N, Guvenc I, Onguru O, et al. The added value of the apparent diffusion coefficient calculation to magnetic resonance imaging in the differentiation and grading of malignant brain tumors. *J Comput Assist Tomogr*. 2004;28(6):735–746.
11. Bulakbasi N, Kocaoglu M, Ors F, et al. Combination of single-voxel proton MR spectroscopy and apparent diffusion coefficient calculation in the evaluation of common brain tumors. *AJNR Am J Neuroradiol*. 2003;24(2):225–233.
12. Higano S, Yun X, Kumabe T, et al. Malignant astrocytic tumors: clinical importance of apparent diffusion coefficient in prediction of grade and prognosis. *Radiology*. 2006 Dec;241(3):839–846.
13. Lee E, terBrugge K, Mikulis, et al. Diagnostic value of peritumoral minimum apparent diffusion coefficient for differentiation of glioblastoma multiforme from solitary metastatic lesions. *AJR Am J Roentgenol*. 2011;196:71–76.
14. Durand-Muñoz C, Flores-Alvarez E, Moreno-Jimenez S, Roldan-Valadez E. Pre-operative apparent diffusion coefficient values and tumour region volumes as prognostic biomarkers in glioblastoma: correlation and progression-free survival analyses. *Insights Imag*. 2019 Mar 18;10(1):36.
15. Daumas-Duport C, Varlet P, Bacha S, Beu-von F, et al. Dysembryoplastic neuroepithelial tumors: nonspecific histological forms—a study of 40 cases. *J Neuro Oncol*. 1999;41:267–280.
16. Svolos P, Kousi E, Kapsalaki E, et al. The role of diffusion and perfusion weighted imaging in the differential diagnosis of cerebral tumors: a review and future perspectives. *Tumour characterisation*. *Cancer Imag*. 2014;14:20.
17. Gassenmaier S, Tziflikas I, Fuchs J, et al. Feasibility and possible value of quantitative semi-automated diffusion weighted imaging volumetry of neuroblastic tumors. *Cancer Imag*. 2020 Dec 17;20(1):89.
18. Louis DN, Perry A, Wesseling P, et al. The 2021 WHO classification of tumors of the central nervous system: a summary. *Neuro Oncol*. 2021 Aug 2;23(8):1231–1251.